Critical exponents of the driven elastic string in a disordered medium

Olaf Duemmer* and Werner Krauth†
CNRS-Laboratoire de Physique Statistique, Ecole Normale Supérieure, 24 rue Lhomond, 75231 Paris Cedex 05, France
(Received 31 January 2005; revised manuscript received 12 April 2005; published 16 June 2005)

We analyze the harmonic elastic string driven through a continuous random potential above the depinning threshold. The velocity exponent $\beta=0.33(2)$ is calculated. We observe a crossover in the roughness exponent ζ from the critical value 1.26 to the asymptotic (large force) value of 0.5. We calculate directly the velocity correlation function and the corresponding correlation length exponent $\nu=1.29(5)$, which obeys the scaling relation $\nu=1/(2-\zeta)$, and agrees with ν_{FS}, the finite-size-scaling exponent of fluctuations in the critical force. Surprisingly, the velocity correlation function is nonuniversal at short distances.

DOI: 10.1103/PhysRevE.71.061601 PACS number(s): 64.60.−i, 05.70.Ln, 68.08.−p

Driven elastic manifolds in disordered media model the physics of systems as diverse as charge density waves [1], interfaces in disordered magnets [2], contact lines of liquid menisci on rough substrates [3], vortices in type-II superconductors [4] and crack propagation in solids [5].

An elastic manifold, driven through disorder by an external force, undergoes a dynamic phase transition [6] that arises from competition between the driving force and the pinning energy due to the disorder, mediated by the elasticity of the manifold. Analogous to an equilibrium phase transition, the driving force acts as the control parameter, and the average center-of-mass velocity v of the manifold acts as order parameter. Two phases of respectively zero and nonzero order parameter are separated by the critical force f_c. At forces below this depinning threshold f_c, the disorder "pins" the manifold and for long enough times, the velocity of the manifold is zero. Above f_c, the manifold continues to advance in avalanches. When the threshold is approached from above ($f \to f_c^+$), the mean velocity tends to zero, and typical length, width and duration of the avalanches diverge. This critical divergence is characterized by two independent scaling exponents.

Much effort [7–10] has been spent on calculating the universal exponents, particularly for driven elastic manifolds in the limit of quasi-static motion. In this limit, inertial terms are neglected and the force acting on the manifold is assumed independent of velocity. The net force on the manifold comprises a constant driving force f, a position-dependent random force η and an elastic restoring force. Choosing a harmonic short range elastic force leads to the following equation of motion for the manifold h at zero temperature

$$\partial_t h(x,t) = f + \eta(x,h(x,t)) + \partial_x^2 h(x,t). \qquad (1)$$

In general, the manifold is represented as a single-valued function $h(x,t)$ defined over a D-dimensional transversal space x, moving in a $(D+1)$-dimensional disorder. In this paper, we consider one discrete dimension $D=1$ with periodic boundary conditions for the string of length L ($x+L$ is identified with x) and for the disorder of lateral extension M ($h+M$ is identified with h, up to a winding term). The continuous disorder of unit strength and unit correlation range is constructed like in [11].

In what follows, we numerically investigate the dynamics of the $(1+1)$-dimensional string above the depinning threshold. Convergence of the dynamical solution is ensured by exploiting the particular analytical structure [12,13] of the equation of motion: it has a unique periodic solution for each disorder sample in the $t \to \infty$ limit. Having found this unique periodic solution, we are thus certain to have reached the asymptotic regime and to have shaken off all influence of arbitrary initial conditions. The asymptotic periodic solution for each disorder sample is constructed to desired precision using a continuous integration routine for Eq. (1). Averaging observables over one period and over disorder samples, we calculate the velocity exponent β and describe in detail how the correlation length diverges as $f \to f_c^+$.

In the thermodynamic limit, the string velocity obeys a power law: $v \sim (f-f_c)^\beta$ for $f \to f_c$. On finite systems, the critical force f_c^{smpl} fluctuates from sample to sample, putting a limit on how small the control parameter $f-\langle f_c^{\mathrm{smpl}}\rangle$ can be made without introducing undesired corrections to scaling relations; a limit from which previous numerical calculations suffer [8,14].

We are able to determine the exact sample-dependent depinning threshold f_c^{smpl} thanks to a recent algorithm [15]. The sample critical force itself shows non-negligible fluctuations of the order of $\sigma_{f_c} \approx L^{-1/\nu_{\mathrm{FS}}}$. The algorithm also finds the final critical configuration h_c and the roughness exponent ζ at depinning [11].

Knowing the critical force f_c^{smpl} of each sample, we plot the time- and disorder-averaged velocity v against $f-f_c^{\mathrm{smpl}}$. Thus we eliminate the statistical noise due to the fluctuating critical force, and obtain extraordinarily clean data. Furthermore, the control parameter $f-f_c^{\mathrm{smpl}}$ can be made arbitrarily small, which is not possible when using $f-\langle f_c^{\mathrm{smpl}}\rangle$.

The mean velocity on a *finite* sample shows three different regimes (see Fig. 1): For very small $f-f_c^{\mathrm{smpl}}$, the motion of the entire string is correlated, and it behaves effectively like a single particle [$v \sim (f-f_c^{\mathrm{smpl}})^{1/2}$]. At intermediate forces, the

*Electronic address: duemmer@lps.ens.fr
†Electronic address: krauth@lps.ens.fr; URL: http://www.lps.ens.fr/~krauth

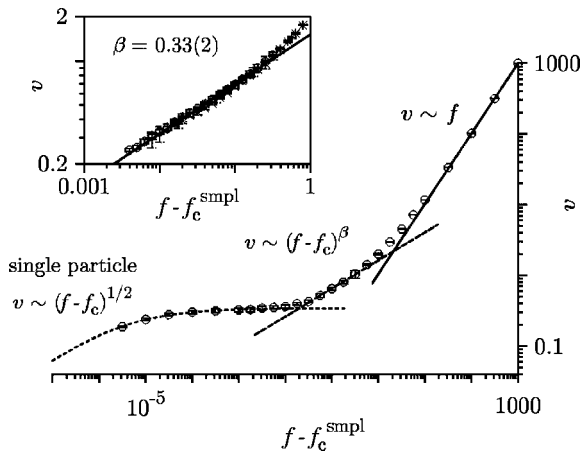

FIG. 1. Mean velocity v of the elastic string vs $f-f_c^{\mathrm{smpl}}$ ($L=128$, $M=195$, 18 samples). The window of critical power law behavior is sandwiched between the single-particle regime $v \sim f^{1/2}$ at very small $f-f_c^{\mathrm{smpl}}$—fitted to Eq. (2)—and linear $v \sim f$ behavior at large f. Inset: critical window for larger system sizes $L=512, \ldots, 2048$ with $M \sim L^{\zeta}$. Slope on log-log plot yields the velocity exponent $\beta=0.33(2)$.

string is correlated on length-scales ξ and moves collectively $[v \sim (f-f_c^{\mathrm{smpl}})^{\beta}]$. At high forces the motion is essentially uncorrelated ($v \sim f$).

At $f=f_c^{\mathrm{smpl}}$, the finite dynamical system [Eq. (1)] (in the $t \to \infty$ limit) undergoes a saddle node bifurcation between a static (pinned) and a periodic (depinned) solution; the global velocity minimum changes from stable to unstable. For very small positive $f-f_c^{\mathrm{smpl}}$, the string spends the major part of its time-period passing through the velocity minimum, and negligibly little time completing its orbit. The motion through the minimum is dominated by the mode $\tilde{h}$ with the largest eigenvalue in a linear stability analysis around the critical configuration h_c. The mode $\tilde{h}$ moves at a velocity equal to $f-f_c^{\mathrm{smpl}}$ plus quadratic and higher corrections in $\tilde{h}$. Hence we can express the time spent inside the minimum as: $\int (dh/v) = \int [dh/(f-f_c^{\mathrm{smpl}}+c\tilde{h}^2)] = T_i (f-f_c^{\mathrm{smpl}})^{-1/2}$, to first order in $f-f_c^{\mathrm{smpl}}$. The remaining time T_o spent outside the velocity minimum depends only weakly on $f-f_c^{\mathrm{smpl}}$. This yields for the velocity as a function of force:

$$M/v = T = T_o + T_i (f - f_c^{\mathrm{smpl}})^{-1/2}. \tag{2}$$

As shown in Fig. 1, this function—combining the effective single-particle exponent one half $[v \sim (f-f_c^{\mathrm{smpl}})^{1/2}]$ for very small forces with the saturation at slightly larger forces—fits the data perfectly.

At intermediate forces, the dynamics leave the single-particle regime and enter the regime of critical collective motion. The crossover takes place when the dynamic correlation length ξ, which diverges as $\xi \sim (f-f_c)^{-\nu}$, equals the system size L [16]. It follows that the difference between the corresponding crossover force and the sample critical force scales as $L^{-1/\nu}$. This scaling is quite slow because of the small exponent $1/\nu \approx 0.7$, as our data confirms. The other crossover, between the critical region and the linear regime, is independent of system size.

Between the two crossovers lies the window of collective behavior, small and slowly growing with L: Only strings of length $L \gtrsim 512$ show any significant evidence for critical behavior, and even for $L=2048$ (see inset of Fig. 1) the window is less than two decades. These pronounced finite-sample-size effects limiting the critical window (also observed in the CDW model [17]) could obscure critical behavior in experimental situations. For example, in an experiment of a liquid-solid contact line advancing on a disordered substrate [18] the sample size, i.e. the capillary length acting as upper cutoff, is $L \approx 200$ in units of the disorder correlation length. For these small samples we expect the window of collective behavior to be hardly noticable and finite-size effects to dominate.

When extrapolating data to the thermodynamic limit, we have to carefully choose the lateral sample size: M has to be of the order of the typical width W of a string of length L at depinning. When increasing L, W scales as L^{ζ}, ζ being the roughness exponent. Hence the lateral sample size M has to scale as L^{ζ}, too. Otherwise, if M is scaled with an exponent $\zeta' < \zeta$, the periodic sample is too short, the string wraps around it, and generates correlations which mix in properties of the charge density wave model (CDW, $M \sim 1$), itself member of a different universality class [19]. If on the other hand M scales with $\zeta' > \zeta$, the sample is too long and contains about $M/W \sim L^{\zeta'-\zeta}$ independent critical configurations of size $L \times W$. Each of these configurations has a slightly different *local* critical force, and the critical force of the entire sample is given by their maximum, and not their mean. Consequently the critical force of a sample of size $M \gg W$ overestimates f_c, even in the thermodynamic limit. We therefore use disorder samples with a length of $M \sim L^{\zeta}$ when investigating the mean velocity.

Analyzing the mean velocity inside the window of critical collective behavior, we find $\beta=0.33(2)$ (see inset of Fig. 1). In comparison, β has been determined in the framework of the functional renormalization group, so far the only analytical approach capable of properly treating the critical dynamics of elastic interfaces in random media. One-loop calculations in $\epsilon=D-4$ yield $\beta=1-\epsilon/9$ [7,10], and recent two-loop calculations [9] yield an estimate of $\beta=0.2(2)$. Our value for β also compares well with the one $[\beta=0.35(5)]$ found in a direct Monte Carlo simulation of an advancing magnetic domain wall in a 2D random Ising system [20], showing that complex domain boundary dynamics can be explained by the model of the elastic string in a random potential.

Our value for β is larger than previous numerical estimates on continuous systems 0.22(2) [14] and on automaton models 0.25(3) [10]. In these studies, however, v was plotted against $f-\langle f_c^{\mathrm{smpl}} \rangle$, and β was probably measured partly inside the critical window and partly inside the finite-size-effect region where the velocity saturates, leading to β being underestimated.

At the depinning threshold the typical size ξ of avalanches diverges. Now, if two points on the string take part in the same avalanche, they have correlated instantaneous velocities. Therefore, the typical length of avalanches shows up as

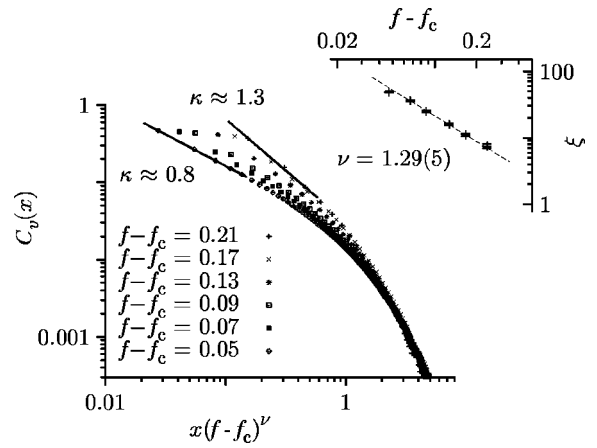

FIG. 2. Connected velocity-velocity correlations $C_v(x)$ for different driving forces $f-f_c$ ($L=512$, $M=20000$, 700 samples). The distance x is rescaled by the correlation length $\xi \sim (f-f_c)^{-\nu}$. Using Eq. (3) as functional template, the correlation function shows a short distance exponent κ depending on $f-f_c$, and thus is nonuniversal. The correlation length ξ and its exponent ν (see inset) are obtained from individual fits.

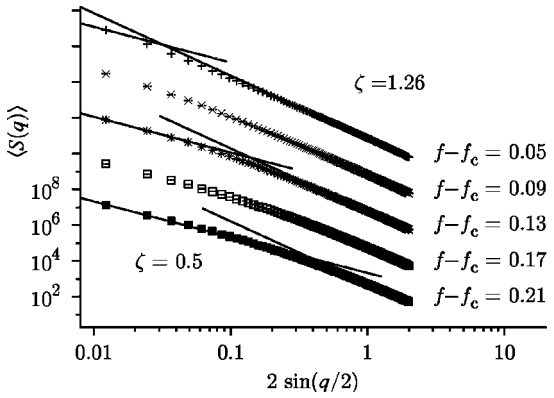

FIG. 3. The structure factor $\langle S(q) \rangle \sim 1/q^{1+2\zeta}$ for different values of $f-f_c$ ($L=512$, $M=20000$, 200 samples). Two regimes of different roughness ζ are visible: At small q values $\zeta=1/2$, while for large q, $\zeta=1.26$. The crossover tends toward zero for $f \to f_c$, illustrating the diverging correlation length. The data is plotted against $2\sin(q/2)$ in order to minimize lattice artifacts. Curves for different $f-f_c$ are offset along the y axis, and lines are guides to the eye.

the characteristic length scale in the velocity correlation function, and diverging avalanch sizes are equivalent to a diverging correlation length ξ.

Whereas previous work did not succeed in accessing ξ directly, we are able to compute this dynamic correlation length from the velocity correlation function and, independently, the structure factor. In our continuous calculation, contrary to automaton models, the instantaneous velocities $v(x,t)$ are readily available, and the velocity correlation function can be computed unequivocally:

$$C_v(x) = \langle v(x)v(0) \rangle_c = \sum_{x'}^{L} \langle [v(x'+x,t) - \overline{v}][v(x',t) - \overline{v}] \rangle_t .$$

We analyze this correlation function $C_v(x)$ by means of the functional form

$$C_v(x) \simeq C_0 x^{-\kappa} e^{-x/\xi} \tag{3}$$

to capture exponential decay on long distances—specified by the correlation length ξ—and algebraic behavior on short distances.

Much to our surprise, the velocity correlations are nonuniversal: the exponent κ characterizing the algebraic short-distance behavior depends on $f-f_c$, unlike previously thought [7,8]. Consequently, the correlation functions $C_v(x)$ for different values of $f-f_c$ cannot be made to collapse on one single master curve [see Fig. 2 for $C_v(x)$ as a function of x/ξ]. The correlation function being nonuniversal makes it also difficult to extract ν—the universal exponent of correlation length divergence—from a scaling plot. We therefore calculate the correlation length ξ by means of individual three-parameter fits of the data to Eq. (3) for given values of $f-f_c$ (see inset of Fig. 2). It is then possible to unambiguously determine the exponent ν that characterizes the correlation length divergence $\xi \sim (f-f_c)^{-\nu}$.

For the correlation length exponent we find a value of $\nu=1.29(5)$ which agrees well with $\nu_{\mathrm{FS}}=1.33(1)$ found in a finite-size-scaling analysis of sample-to-sample fluctuations of the critical force [21]. Hence we confirm that the dynamic correlation length exponent and the finite-size-scaling correlation length exponent are identical $\nu=\nu_{\mathrm{FS}}$ [7,9]. Furthermore, our value for ν obeys the statistical tilt symmetry relation $\nu=1/(2-\zeta)$ [10]. Concerning the nonuniversality of the correlation function, we have not attempted to establish a definite functional relation between κ and $f-f_c$.

An avalanche of typical length ξ has a typical width w which scales like $w \sim \xi^{\zeta}$. As a second method to estimate the roughness exponent ζ, we study the time- and disorder-averaged structure factor $S(q)$, which behaves like $1/q^{1+2\zeta}$, when defined as $S(q)=\langle h(q)h(-q) \rangle_c$ with $h(q)=\Sigma_x^L e^{iqx}h(x)$.

At large driving forces $f \to \infty$, the roughness exponent of the harmonic elastic string is $\zeta=1/2$: The noise due to the disorder becomes equivalent to thermal noise, which can be seen from expanding the disorder term η in the equation of motion [Eq. (1)]—transformed to the center of mass reference frame—in powers of $v^{-1} \approx f^{-1}$, yielding a $\delta(t)$ correlated noise to first order. At depinning, on the other hand, the roughness exponent takes on the value $\zeta=1.26(1)$ [11].

Inside the critical window, both these values for ζ show up in the structure factor, and characterize two different ranges of q separated by the inverse of the correlation length: for large wave vectors ($q \gtrsim 2\pi/\xi$) the structure factor displays the critical roughness, whereas at small wave vectors ($q \lesssim 2\pi/\xi$) it shows the thermal roughness. Figure 3 tracks the crossover between the two regimes as $f \to f_c^+$, illustrating the diverging correlation length ξ. The corresponding correlation length exponent ν is consistent with our value calculated from the velocity correlation function, but less precise.

In our calculation of the correlation function, the lateral size M must be chosen sufficiently large for the string not to notice the periodicity of the disorder—otherwise, the structure factor displays, in addition to the two regimes mentioned, the roughness of a CDW ($\zeta_{\mathrm{CDW}}=3/2$ [19]), in those q modes that have not yet decorrelated after one period. The

mode q decorrelates in a time $\sim q^{-z}$ with z the dynamic exponent. This implies that the smallest mode $2\pi/L$ needs a distance of roughly $L^z \gg L^\zeta (z \approx 1.5)$ to decorrelate. We therefore have to choose a disorder period of $M \gg L^\zeta$ in our analysis of $S(q)$ and $C_v(x)$, in order to eliminate autocorrelation effects in the largest length-scales.

In contrast, in our initial analysis of the mean velocity we were justified in adopting a scaling $M \sim L^\zeta$ because the effective string viscosity—which determines β—is caused by pinning on length scales *below* ξ. The shorter periodicity $M \sim L^\zeta$ thus does not influence the velocity exponent β.

At very large M, the sample critical force f_c^{smpl} becomes too large to be used as the critical force. We therefore calculate a mean critical force f_c^∞ from a finite-size-scaling ansatz: The average sample critical force is taken to depend on the sample length L as $f_c^\infty - \langle f_c^{\mathrm{smpl}}(L) \rangle \sim L^{-1/\nu_{\mathrm{FS}}}$. The asymptotic value $f_c^\infty = 1.913(2)$ is then used as a mean critical force when analyzing the velocity correlations and the structure factor.

When investigating the correlation length ξ directly via $C_v(x)$ and $S(q)$, we do not need to know f_c^{smpl} in order to avoid the crossover from the critical window into the finite-size-effect region: We simply limit our analysis to sufficiently small values of ξ/L. In addition, the smallest value of $f - f_c^\infty$ analyzed is larger than typical fluctuations in f_c^{smpl}, which are therefore negligible.

In conclusion, we analyze the quasistatic dynamics of the harmonic elastic string driven through a random potential, above the depinning transition. We calculate the exact periodic solution for each sample, and encounter large finite-sample-size effects, which will have repercussions in experimental situations. Knowing exactly the sample critical force enables us to identify the limited window of critical collective behavior and to determine the velocity exponent $\beta = 0.33(2)$. We investigate the velocity correlation function, determine the correlation length exponent $\nu = 1.29(5)$, and confirm that it both obeys the statistical tilt symmetry and agrees with the finite-size-scaling correlation length exponent. Surprisingly, we find a nonuniversal functional form for the velocity correlation function: the exponent κ describing the algebraic short distance behavior depends on the control parameter $f - f_c$.

We would like to thank P. Le Doussal, S. Guibert, A. Rosso, and K. Wiese for stimulating discussions.

[1] G. Grüner, Rev. Mod. Phys. **60**, 1129 (1988).
[2] S. Lemerle *et al.*, Phys. Rev. Lett. **80**, 849 (1998).
[3] A. Prevost, E. Rolley, and C. Guthmann, Phys. Rev. B **65**, 064517 (2002).
[4] G. Blatter *et al.*, Rev. Mod. Phys. **66**, 1125 (1994).
[5] H. Gao and J. R. Rice, J. Appl. Mech. **56**, 828 (1989).
[6] D. S. Fisher, Phys. Rev. B **31**, 1396 (1985).
[7] O. Narayan and D. S. Fisher, Phys. Rev. B **48**, 7030 (1993).
[8] M. Dong, M. C. Marchetti, A. A. Middleton, and V. Vinokur, Phys. Rev. Lett. **70**, 662 (1993).
[9] P. Chauve, P. Le Doussal, and K. J. Wiese, Phys. Rev. Lett. **86**, 1785 (2001); P. Le Doussal, K. J. Wiese, and P. Chauve, Phys. Rev. B **66**, 174201 (2002).
[10] T. Nattermann, S. Stepanow, L. H. Tang, and H. Leschhorn, J. Phys. II **2**, 1438 (1992).
[11] A. Rosso, A. K. Hartmann, and W. Krauth, Phys. Rev. E **67**, 021602 (2003); A. Rosso and W. Krauth, Phys. Rev. Lett. **87**, 187002 (2001).
[12] A. A. Middleton, Phys. Rev. Lett. **68**, 670 (1992). A complete proof of Middleton's theorem is contained in [13].
[13] C. Baesens and R. S. MacKay, Nonlinearity **11**, 949 (1998).
[14] F. Lacombe, S. Zapperi, and H. J. Herrmann, Phys. Rev. B **63**, 104104 (2001).
[15] A. Rosso and W. Krauth, Phys. Rev. E **65**, 025101(R) (2002).
[16] *Finite Size Scaling*, edited by J. L. Cardy (North-Holland, New York, 1988).
[17] C. R. Myers and J. P. Sethna, Phys. Rev. B **47**, 11171 (1993).
[18] S. Moulinet, C. Guthmann, and E. Rolley, Eur. Phys. J. E **8**, 437 (2002).
[19] O. Narayan and D. S. Fisher, Phys. Rev. B **46**, 11520 (1992).
[20] U. Nowak and K. D. Usadel, Europhys. Lett. **44**, 634 (1998).
[21] C. J. Bolech and A. Rosso, Phys. Rev. Lett. **93**, 125701 (2004).